ChemPubSoc Europe

DOI: 10.1002/open.201500011

Open Access ChemistryOPEN Full Papers

Solvent-Tuned Self-Assembled Nanostructures of Chiral L/D-Phenylalanine Derivatives of Protoporphyrin IX

Mr. Sharad R. Bobe,[a, c] Mohammad Al Kobaisi,[b] Sheshanath V. Bhosale,*[b] and Sidhanath V. Bhosale*[a]

Protoporphyrin IX is a naturally occurring amphiphilic porphyrin with a rigid hydrophobic nonpolar core and two polar propionic acid substitutions on the porphyrin ring. This molecule can be modified on the hydrophilic group, which can lead to strengthened π–π-stacking and spontaneous self-assembly into novel nanostructures. Herein, we use L- phenylalanine and D-phenylalanine to modify protoporphyrin IX, and use the two derivatives for solvophobic-controlled self-assembly. Both derivatives possess two important features: 1) the aromatic core of the porphyrin for dispersive interactions and 2) a chiral amino acid to maximize the influence of chirality on self-assembly. These derivatives lead to the formation of a variety of nanostructure morphologies, such as spheres, nanofibers, lamellar structures, and thread-like and spherical shells. Solution-based self-assembly was determined by UV/Vis, fluorescence, and circular dichroism spectroscopy, and the formed nanostructures were characterized by scanning electron microscopy (SEM). Such engineered porphyrin derivatives could have potential applications in energy transport and storage, supramolecular chemistry, materials science, and medicine.

Introduction

Protoporphyrin IX (**I**) (Figure 1) is an amphiphilic porphyrin with a rigid hydrophobic nonpolar core, lipophilic substitutions at C2, C3, C7, C8, C12, and C18, and two polar propionic acid substitutions at C13 and C17 in the porphyrin ring.[1] This arrangement prevents crystallization and favors self-aggregation via very stable dimers in which the porphyrin unit rotates by 180° resulting in a symmetric distribution of the hydrophilic head groups.[2] This amphiphilic arrangement can be modified on both the hydrophobic vinyl group, as well as the hydrophilic propionic acid group. The expansion of the planar aromatic core can be employed to construct novel nanostructures by strengthening π–π-stacking and spontaneous self-assembly.

Engineering the protoporphyrin IX and its derivative assemblies to create functional nanomaterials is an attractive field of research due to their various potential applications.[3,4] These materials could be used in long-range energy and electron transport (e.g. light harvesting and mimicking natural photosynthesis),[5–10] supramolecular chemistry,[11–16] materials science,[17,18] solar cells,[19] and biomedical applications.[20–23] In our previous work,[24–27] examples used for self-assembly included alkyl- or oligoethylene-glycol-substituted rings on the polar end or both polar and nonpolar sides (Figure 1). Specifically, the self-assembly of the triethylene-glycol-modified protoporphyrin IX derivative **II** produced uniformly-sized, multilamellar microvesicles in nonpolar solvent mixtures and micellar aggregates in polar solvent mixtures.[24] Protoporphyrin IX derivative **III**, bearing highly branched alkyl chains, self-assembled into well-defined nanostructures, e.g. rod- and honeycomb-like morphologies, in polar and nonpolar solvent mixtures via solvophobic control.[25] The expansion of the hydrophobic region of protoporphyrin IX by substituting with alkyl chains and triethylene glycol at both hydrophilic and hydrophobic ends, respectively, resulted in compound **IV**, which aggregated into long nanowires.[26] Finally, fibril nanostructures were produced when hydrophobic alkyl chains were substituted on one end and triethylene glycol in the hydrophilic region of protoporphyrin IX derivative **V**.[27]

In nature, elegant arrangements of peptide–porphyrin conjugates are essential in conducting biological processes.[28–31] This has inspired researchers worldwide to investigate the self-assembly and supramolecular structures of porphyrin–peptide conjugates mimicking the structure and role of natural porphyrin.[32–38] In this work, we explore the development and use of L- and D-phenylalanine-substituted protoporphyrin IX derivatives **1** and **2**, respectively, for the solvophobic-controlled assembly of nanostructures (Figure 2). Characteristically, L- and D-phenylalanine-substituted protoporphyrin IX derivatives **1** and

[a] M. S. R. Bobe, Dr. S. V. Bhosale
Polymers and Functional Material Division, CSIR-Indian Institute of Chemical Technology, Hyderabad, Telangana 500 007 (India)
E-mail: bhosale@iict.res.in

[b] Dr. M. Al Kobaisi, S. V. Bhosale
School of Applied Sciences, RMIT University
GPO Box 2476, Melbourne, VIC 3001 (Australia)
E-mail: sheshanath.bhosale@rmit.edu.au

[c] M. S. R. Bobe
Department of Organic Chemistry, School of Chemical Sciences
North Maharashtra University, Jalgaon, M.S. 425 001 (India)

Supporting information for this article is available on the WWW under http://dx.doi.org/10.1002/open.201500011.

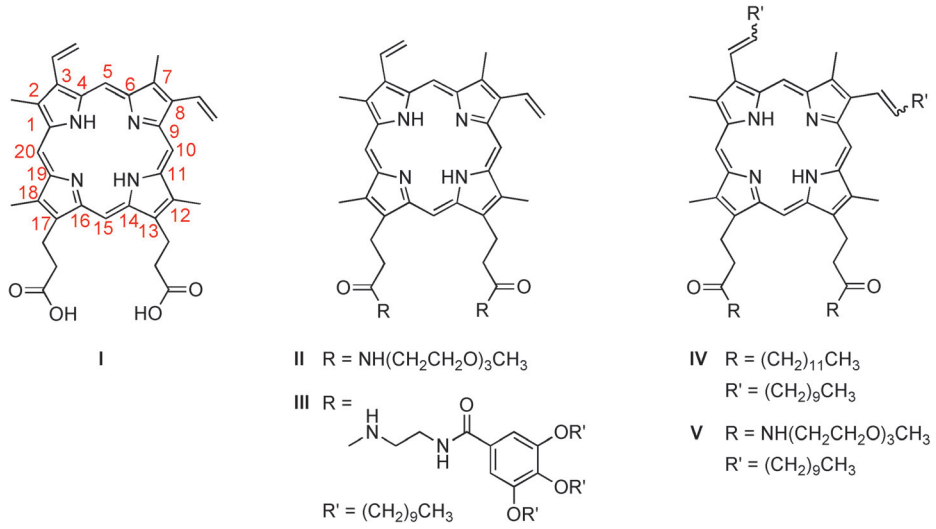

Figure 1. Substituted protoporphyrin IX derivatives **I–V** reported with self-assembly capabilities.

Results and Discussion

Synthesis

The protoporphyrin IX derivatives modified with L- and D-phenylalanine (compounds **1** and **2**) were prepared in two steps:[39] The first step was formation of diacetyl chloride from the reaction of commercially available protoporphyrin IX and oxalyl chloride in dry dichloromethane under nitrogen for four hours. Next, protoporphyrin IX diacetyl chloride was readily reacted with methyl L- or D-phenylalanine hydrochloride salt

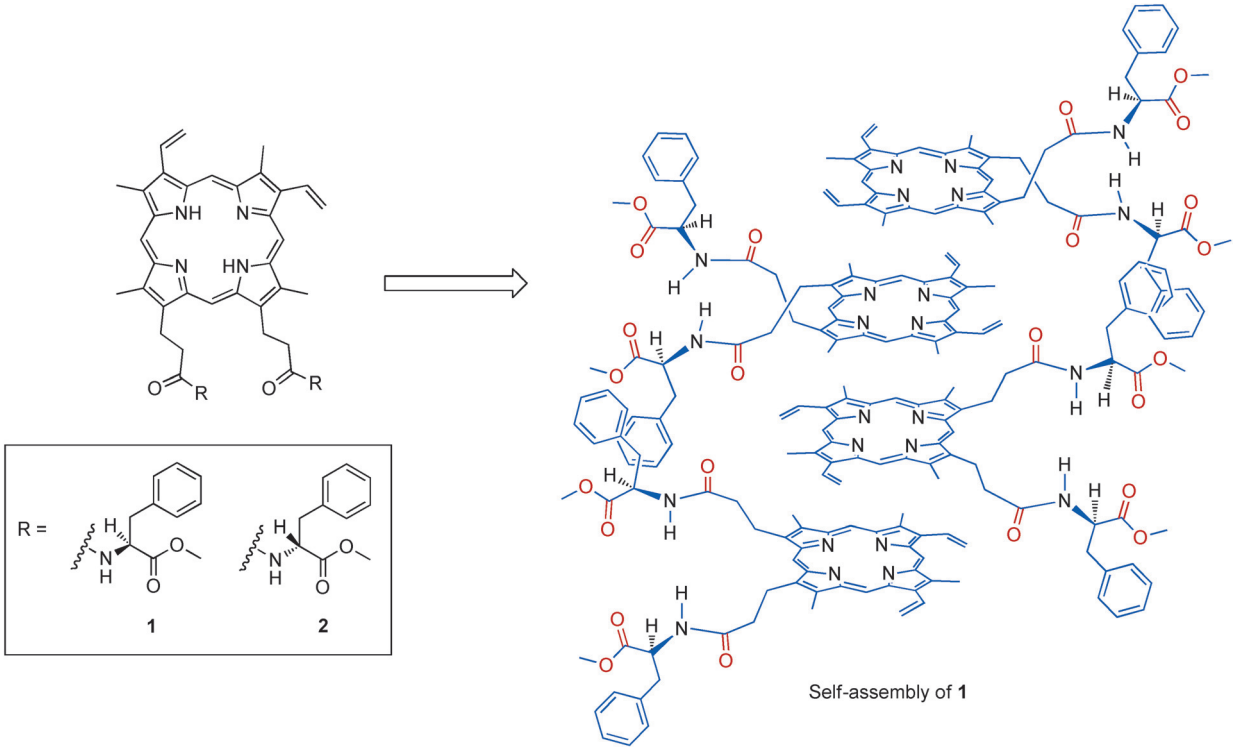

Figure 2. Structures of L- and D-phenylalanine-substituted protoporphyrin IX derivatives **1** and **2** and a scheme proposing the self-assembled structure of **1** in a fibril network.

2 possess two important properties resulting in the formation of varied nanostructures through noncovalent interactions: 1) a porphyrin aromatic core which is designed to optimize the dispersive interactions (π—π stacking and van der Waals interactions) between the cores within a construct and 2) a chiral amino acid that helps maximize the influence of solvents and chirality in aggregation mode.

using a catalytic amount of pyridine in dry dichloromethane, under nitrogen atmosphere. These reactions gave **1** and **2** as a purple solids in quantitative yields (Scheme 1). Compounds **1** and **2** were fully characterized using infrared (IR) spectroscopy, ^{1}H and ^{13}C NMR spectroscopy, and electrospray ionization (ESI) and high-resolution mass spectrometry (HRMS). Their optical properties were measured by UV/Vis, fluorescence, and circular dichroism (CD) spectroscopy.

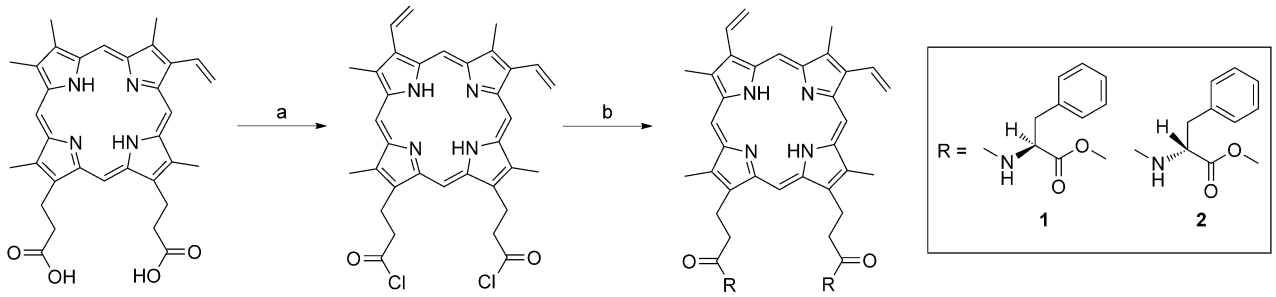

Scheme 1. Synthesis of protoporphyrin IX derivatives **1** and **2**. *Reagents and conditions*: a) $COCl_2$, dry CH_2Cl_2, N_2, rt, 4 h; b) L- or D-phenylalanine hydrochloride salt, dry CH_2Cl_2, catalytic amount of pyridine, rt, 24 h, 80% (**1** or **2**).

UV/Vis absorption and fluorescence spectroscopy

1 and **2** were found to be well soluble in chloroform resulting in a sharp absorption spectra consistent with the presence of the monomeric form.[24–27] Typically, the absorption spectrum of **1** in chloroform showed a Soret band at 408 nm ($\varepsilon = 4.1 \times 10^5\ M^{-1}\,cm^{-1}$) and four weaker Q-bands at 505, 541, 576, and 630 nm (Figure 3).

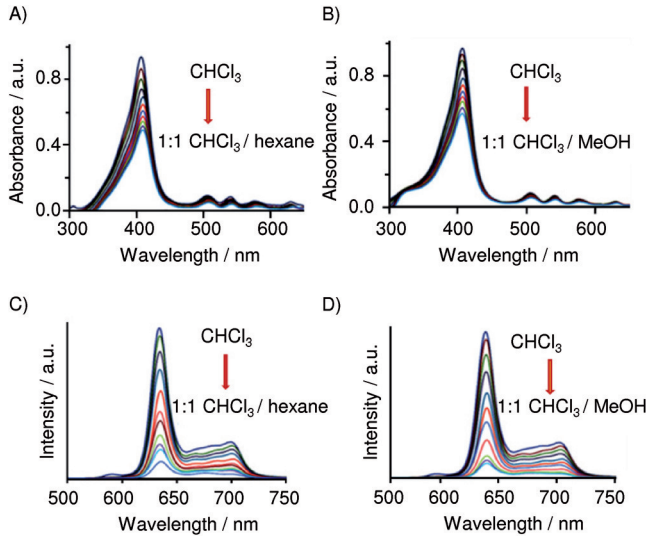

Figure 3. A—B) UV/Vis absorption spectra of **1** (1×10^{-5} M) in $CHCl_3$/hexane (A) and $CHCl_3$/MeOH (B). C—D) Fluorescence emission spectra ($\lambda_{ex} = 408$ nm) of **1** in $CHCl_3$/hexane (C) and $CHCl_3$/MeOH (D).

Changing the hexane to chloroform ratios of solutions of **1** conferred significant changes in its UV/Vis absorption bands. The changes could be attributed to aggregation effects leading to a reduction in the peak intensity, along with a 3 nm red-shift of the Soret band and a loss of the fine structure. The absorption of **1** in chloroform/methanol showed almost identical behavior to the spectrum in chloroform/hexane, except for the absence of the red shift at $\lambda_{max} = 408$ nm (Figure 3B). This phenomenon is associated with J-type aggregation. Temperature-dependent UV/Vis absorption spectroscopy of compounds **1** and **2** revealed that in chloroform/hexane, disaggregation happens above 40 °C, whereas in chloroform/methanol, the self-assembly destabilizes above 50 °C (see Figures S1 and S2 in the Supporting Information). Competitive experiments with H-bond-displacing solvents, like dimethylsulfoxide (DMSO), showed the disaggregation of the assembly with a slightly decreased absorption intensity only due to dilution effects (Figures S3 and S4 in the Supporting Information). Furthermore, concentration-dependent UV/Vis absorption spectroscopy only showed increasing intensities for both compounds **1** and **2** (Figures S5 and S6 in the Supporting Information).

The emission spectrum of **1** in chloroform showed two bands at 633 and 701 nm upon excitation at 408 nm (Figure 3C). The aggregation features of **1** in solution were studied by varying the proportion of hexane in chloroform (0–50% *v/v*). It could be clearly seen that as the proportion of hexane increased, the fluorescence emission of **1** decreased and became red-shifted. An identical trend of fluorescence quenching was observed for **1** in chloroform/methanol (0–50% *v/v*) (Figure 3D). Fluorescence spectroscopy of **1** in chloroform/hexane and chloroform/methanol also supported J-type aggregation.[10–13] The aggregation of compound **2** was also studied using UV/Vis and fluorescence spectroscopy and a similar trend was observed (Figure S7 in the Supporting Information). ^1H NMR spectroscopy of **1** showed broadening of peaks with increasing concentration, which we believe is due to higher aggregates (Figure S8 in the Supporting Information).

CD spectroscopy

The effects of the chirality of **1** and **2** on the self-assembly process were further elucidated by using CD spectroscopy. The L/D-phenylalanine subunit contains a chiral center that can affect the orientation of the self-assembling molecules. What happens is a change in the direction of approach between the hydrogen bonds of aggregating molecules. Here, one would expect protoporphyrin IX derivatives **1** and **2**, appended with L- and D-phenylalanine, to form chiral self-assemblies. The chloroform solutions of **1** and **2** were CD active with characteristic CD spectra (Figure 4). Derivative **1**, bearing an L-phenylalanine amide, showed a bisignated Cotton effect in the range of 350 to 420 nm; that is, symmetric positive bands were observed at 408 nm, a negative band at 418 nm, and a small band at 376 nm. All these correspond to the Soret band of the absorption spectrum of **1**. Thus, the CD spectrum of **1** in chloroform showed positive excitonic Cotton effects, while de-

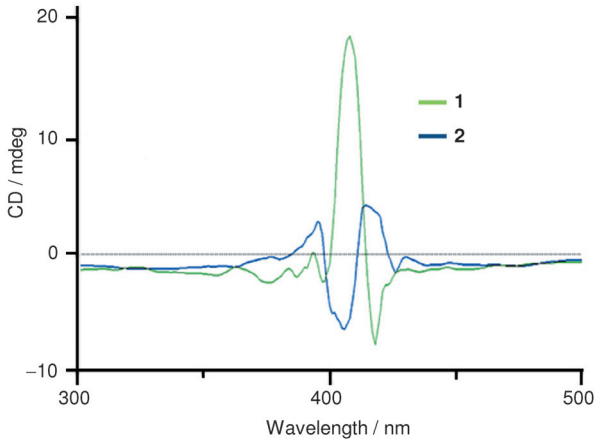

Figure 4. CD spectra of **1** (1×10^{-5} M, green line) and **2** (1×10^{-5} M, blue line) in $CHCl_3$.

rivative **2**, bearing D-phenylalanine amide, showed an asymmetric positive band at 414 nm and a negative one at 406 nm in chloroform. A positive Cotton effect was observed for **1**, and a negative Cotton effect was observed for **2**, indicating P- and M-type helical assembly, respectively.[40,41]

Furthermore, we investigated the effects of nonpolar (hexane) and polar (methanol) solvents on the CD spectra of **1** and **2** in chloroform (Figures S9 and S10 in the Supporting Information). Increasing the hexane proportion decreased the amplitude of the CD signal, causing CD silence at more than 70% hexane. Here, we postulate that at higher proportions of hexane, the increased hydrophobic forces decrease the angles between transition dipole moments of the stacked porphyrins to zero, resulting in CD silencing. A similar trend was also observed upon adding methanol to the chloroform solution. The CD spectra imply that with higher concentrations of **1** and **2**, there are no changes in the Cotton effect. However, after dilution there is a decrease in peak intensity, with the amplitude of the CD signal approaching zero, suggesting probable CD silencing (see Figure S11 in the Supporting Information).

Scanning electron microscopy

Scanning electron microscopy (SEM) was used to visualize the larger nano- and microstructures of the aggregates of **1** and **2** upon evaporation of their solutions in chloroform/hexane (6:4) and chloroform/methanol (6:4) (Figure 5 and Figures S12–S15 in the Supporting Information).

The scanning electron micrograph of **1** in chloroform/hexane (6:4, *v/v*) is shown in Figure 5 A–C. The smallest structures of aggregated **1** from chloroform/hexane were long and thread-like, with 7 nm thickness as shown in Figure 5 C. These threads formed bundles measuring 14 nm in diameter or more, depending on the number of twisted threads aligned along one other. These high-aspect-ratio threads aggregated to form yarns above 200 nm in diameter, e.g. the one shown in Figure 5 B is 310 nm in diameter.

The aggregation structures of **2** in chloroform/hexane (6:4, *v/v*) after solvent evaporation were global agglomerates of irregular smaller structures about 200 nm in diameter with low aspect ratios. Smaller nanostructures were not detected as shown in Figure 5 D–F.

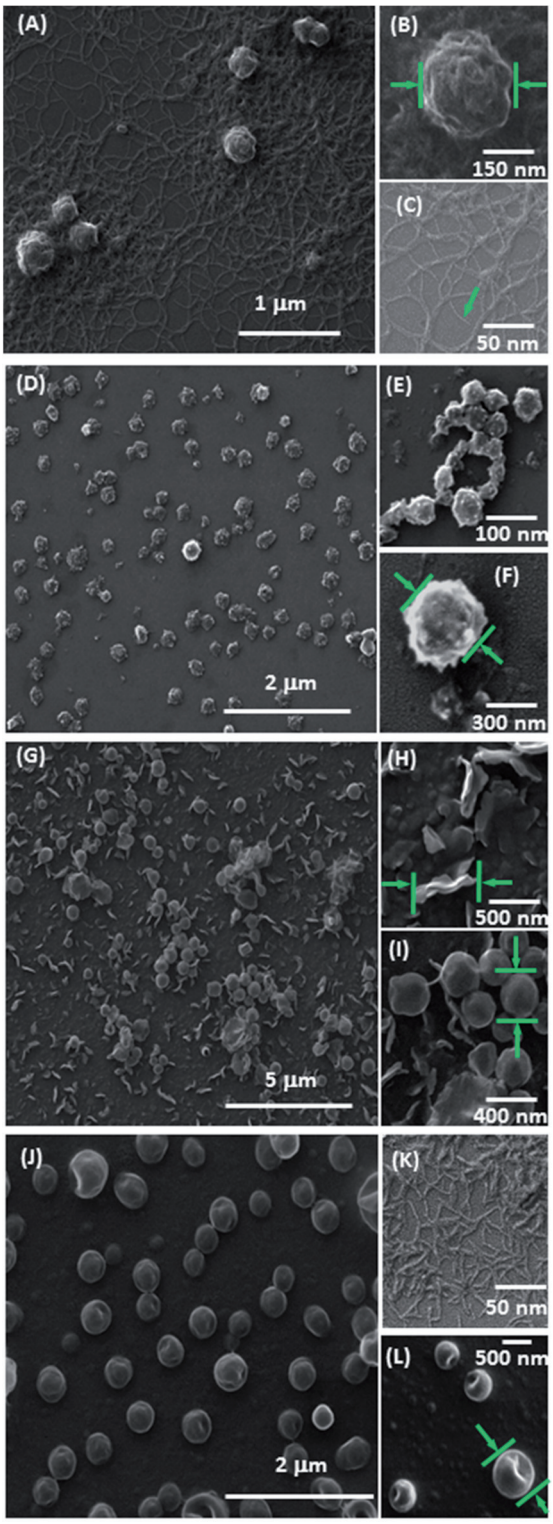

Figure 5. SEM images of aggregates of protoporphyrin IX derivatives (1×10^{-5} M) produced by solvent evaporation. A—C) **1** from $CHCl_3$/hexane (6:4). D–F) **2** from $CHCl_3$/hexane (6:4). G–I) **1** from $CHCl_3$/MeOH (6:4). J–L) **2** from $CHCl_3$/MeOH (6:4).

The aggregation of **1** in chloroform/methanol (6:4, *v/v*) presented two types of large formations: irregular lamellar structures with an average length of 650 nm, as shown in Figure 5H, and spherical shapes with an average diameter of 560 nm, as shown in Figure 5I. Maybe these spherical structures were deformed because they were shells that could not support the structure and buckled under pressure after solvent evaporation. No smaller nanostructures were seen.

The aggregation of **2** in chloroform/methanol (6:4, *v/v*) gave small twisted needle-shaped nanostructures which were, on average, 8 nm wide and 100 nm long as shown in Figure 5K. The main aggregates were larger spherical shells with an average diameter of 500 nm as shown in Figure 5L; these shells collapsed upon solvent evaporation.

Such a solvent-assisted molecular assembly of L-/D-phenylalanine amide allowed us to fabricate various nanostructures, suggesting that the polarity of the solvent plays an important role. This was similar to previously observed controlled nanomorphologies of porphyrin and other derivatives.[42–45] In addition, the presence of the L-/D-phenylalanine group in **1** and **2** favors the induction of chirality in the molecule as shown by CD spectroscopy in Figure 4 and the SEM results, showing twisted needles and thread-like nanostructures which support chirality. However, there were no aggregates of **1** and **2** at any concentration in neat chloroform.

The formation of globular aggregates in solution was confirmed by dynamic light scattering (DLS) analysis of **1** and **2** (1×10^{-4} M). The average diameter was observed to be 100–220 nm with a polydispersity index of 0.11 from chloroform/hexane (6:4, *v/v*), shown in Figure 6. The diameter of the aggregates formed from chloroform/methanol (6:4, *v/v*) fell in the range of 500–850 nm. From this size organization, **1** and **2** in chloroform/methanol (6:4, *v/v*) formed multilamellar spherical shells. Moreover, the globular aggregates displayed a very narrow size distribution, and were highly stable against coagulation. The hydrodynamic radius (R_H) of the vesicles derived from the characteristic line width were obtained by the CONTIN analysis method.[46]

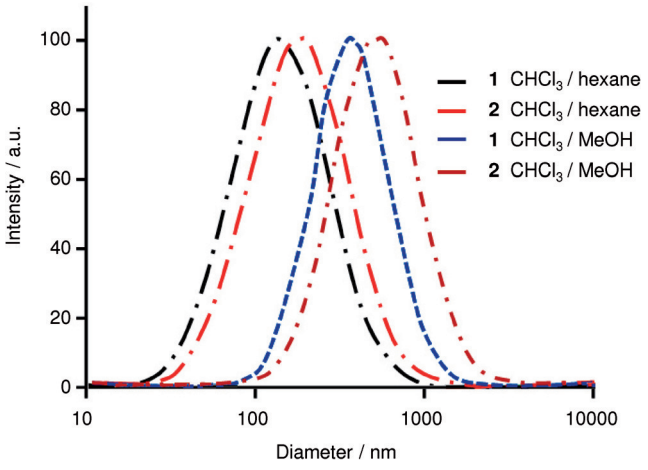

Figure 6. Dynamic light scattering (DLS) analysis of protoporphyrin IX derivative aggregates produced from **1** or **2** (1×10^{-4} M) in $CHCl_3$/hexane (6:4) (left pair) or $CHCl_3$/MeOH (6:4) (right pair).

We speculate that the self-assembly is predominantly driven by π–π interactions among the cores of the porphyrins, with the chiral amino acid interactions leading to further aggregation (Figure 2).The overall structure may also be stabilized by the intermolecular H-bonds between the amide groups of the amino acids.

Conclusions

In summary, we have reported the assembly of protoporphyrin IX derivatives with L-/D-phenylalanine. The fabrication of self-assembled materials is solvent dependent. The results obtained by varying the ratios of solvents such as chloroform/hexane and chloroform/methane, demonstrate that the aggregation of **1** in these solvents forms spherical and fibril nanostructures, and the aggregation of **2** forms fibril bundles with spherical shells and lamellar nanostructures.

Experimental Section

Chemistry

Materials: Protoporphyrin IX, dimethylformamide (DMF), $CHCl_3$, MeOH, and CH_2Cl_2 were purchased from Sigma–Aldrich (Bangalore, India) and used without purification. UV/Vis absorption spectra were recorded on a Shimadzu UV-3150 spectrometer (Kyoto, Japan) and fluorescence emission spectra on a FluoroMax 4 (Horiba Scientific, Kyoto, Japan). ^{1}H NMR (400 MHz) and ^{13}C NMR (100 MHz) spectra were recorded on an Avance 400 NMR spectrometer (Bruker, Billerica, USA) using $CDCl_3$ as solvent. The solvents for spectroscopic studies were of spectroscopic grade and used as received. A stock solution of **1** and **2** was prepared in $CHCl_3$, and self-assembled samples were prepared by diluting these stock solutions with hexane or MeOH. The sample solutions were kept at rt for a few hours before SEM measurement.

UV/Vis spectroscopy: Solutions of **1** and **2** in $CHCl_3$/hexane and $CHCl_3$/MeOH (1×10^{-5} M final concentration) were used to obtain spectra. The UV/Vis measurements were recorded at rt using a Shimadzu UV-3150 spectrophotometer equipped with a cuvette with a path length of 1 cm.

Fluorescence spectroscopy: The fluorescence spectra of derivatives **1** and **2** in $CHCl_3$/hexane and $CHCl_3$/MeOH were taken in a quartz cuvette of 1 mm path length at rt and $\lambda_{ex}=408$ nm. The fluorescence spectra were recorded on a Horiba FluoroMax-4 spectrofluorometer at 25 °C.

CD spectroscopy: CD experiments were performed on a JASCO 815 CD Spectropolarimeter (Tokyo, Japan).

SEM: SEM samples were prepared by solvent evaporation on a silicon wafer and then sputter coating with gold for 10 s at 0.016 mA Ar plasma (SPI, West Chester, USA). These were imaged using an FEI Nova NanoSEM (Hillsboro, USA) operating under high vacuum.

Synthesis of methyl L-phenylalanine diamideprotoporphyrin IX (1): A round-bottom flask containing protoporphyrin IX (100 mg, 0.017 mmol) and dry CH_2Cl_2 (15 mL) was evacuated and flushed with N_2. Then oxalyl chloride (1 mL, 0.08 mmol) was added to the flask dropwise at 0 °C. The reaction mixture was returned to rt and stirred for 3 h. The mixture was then concentrated in vacuo to give

a green solid. The green solid was used without purification for further reaction. L-phenylalanine hydrochloride salt (146 mg, 0.068 mmol) dissolved in dry CH_2Cl_2 (5 mL) was added to a solution of the previously obtained compound in dry CH_2Cl_2 (10 mL). To this reaction mixture pyridine (1 mL) was added dropwise with stirring. The reaction mixture was stirred at rt for 12 h. Then MeOH (5 mL) was added and stirred well for another 5 min. After completion of the reaction (monitored by TLC), the solvent was removed in vacuo. The gummy reaction mixture was dissolved in CH_2Cl_2 (100 mL) and washed with aqueous 10% *w/v* $NaHCO_3$ solution (2× 30 mL), 0.1 M HCl (1×20 mL), H_2O (1×20 mL), and brine (1×20 mL). The resultant organic solvent was dried over Na_2SO4, filtered, and concentrated in vacuo. The resulting solid was purified by flash column chromatography on silica with 1% MeOH in $CHCl_3$ as eluent to give **1** as a dark violet crystalline material (127 mg, 80%); mp: 245 °C; ^{1}H NMR ($CDCl_3$, 400 MHz): δ = 10.09–9.90 (m, 4H, 4× methine protons), 8.20 (m, 2H, 2×$CHCH_2$), 6.80–6.89 (br s, 2H, –CONH), 6.45–6.68 (m, 10H, 5×2 Ph), 6.45–6.15 (m, 4H, 2× $CHCH_2$), 4.62–4.66 (m, 2H, CO–CH–NH), 4.35–4.30 (m, 4H, 2× CH_2CH_2CONH), 3.56–3.66 (m, 12H, 4×ring methyl), 3.14–3.16 (br, s, 6H, 2×OCH_3), 3.00–3.11 (m, 4H, CH_2–Ph), 2.67–2.53 (m, 4H, 2× CH_2CH_2CONH), −3.89 ppm (br s, 2H, 2×ring NH); ^{13}C NMR ($CDCl_3$, 100 MHz): δ = 172.5, 171.6, 135.5, 135.4, 130.1, 128.7, 128.6, 127.8, 126.4, 120.5, 97.6, 96.9, 96.8, 96.6, 53.1, 53.1, 51.7, 39.6, 39.5, 37.3, 37.4, 22.9, 22.8, 12.5, 11.5, 11.4 ppm; IR (KBr): $\tilde{\nu}$ = 1741, 1645, 1539, 1437, 1250, 1108, 1071, 988, 908, 838, 700, 490 cm^{-1}; ESI-MS *m/z*: 885 $[M]^+$; HRMS *m/z* $[M]^+$calcd for $C_{54}H_{56}N_6O_6$: 885.4334, found 885.4349.

Synthesis of methyl D-phenylalanine diamideprotoporphyrin IX (2): Compound **2** was prepared from protoporphyrin IX (100 mg, 0.017 mmol) and D-phenylalanine hydrochloride salt (146 mg, 0.068 mmol) in a similar manner to **1**, to yield a dark violet crystalline material (127 mg, 80%); mp: 250 °C; ^{1}H NMR ($CDCl_3$, 400 MHz): δ = 10.15–9.96 (m, 4H, 4×methine protons), 8.22–8.28 (m, 2H, 2× $CHCH_2$), 6.80–6.87 (br s, 2H, –CONH), 6.45–6.72 (m, 10H, 5×2 Ph), 6.45–6.15 (m, 4H, 2×$CHCH_2$), 4.62–4.66 (m, 2H, CO–CH–NH), 4.35–4.30 (m, 4H, 2×CH_2CH_2CONH), 3.56–3.66 (m, 12H, 4×ring methyl), 3.14–3.16 (br, s, 6H, 2×OCH_3), 3.00–3.11 (m, 4H, CH_2–Ph), 2.67–2.53 (m, 4H, 2×CH_2CH_2CONH), −3.89 ppm (br s, 2H, 2×ring NH); ^{13}C NMR ($CDCl_3$, 100 MHz): δ = 172.5, 171.6, 135.5, 135.4, 130.1, 128.7, 128.6, 127.8, 126.4, 120.5, 97.6, 96.9, 96.8, 96.6, 53.1, 53.1, 51.7, 39.6, 39.5, 37.3, 37.4, 22.9, 22.8, 12.5, 11.5, 11.4 ppm; IR (KBr): $\tilde{\nu}$ = 1741, 1645, 1539, 1437, 1250, 1108, 1071, 988, 908, 838, 700, 490 cm^{-1}; ESI-MS *m/z* 885 $[M]^+$, HRMS: *m/z* $[M]^+$ calcd for $C_{54}H_{56}N_6O_6$: 885.4334, found 885.4356.

Acknowledgements

S. V. B. is grateful for financial support from the Department of Atomic Energy—Board of Research in Nuclear Science (DAE-BRNS), Mumbai (Project Code: 37(2)/14/08/2014-BRNS) and the Council of Scientific and Industrial Research (CSIR), New Delhi, under the Intelcoat Research Program (CSC 0014). S. V. B. (RMIT) acknowledges financial support from the Australian Research Council under a Future Fellowship Scheme (FT110100152) and the RMIT Microscopy and Microanalysis Facility (RMMF). S. R. B. acknowledges the CSIR and the Government of India for senior research fellowship support.

Keywords: chiral aggregates · porphyrins · protoporphyrin IX · nanostructures · supramolecular self-assembly

[1] I. Inamura, K. Uchida, *Bull. Chem. Soc. Jpn.* **1991**, *64*, 2005.
[2] J.-H. Fuhrhop, C. Demoulin, C. Boettcher, J. Koning, U. Siggels, *J. Am. Chem. Soc.* **1992**, *114*, 4159.
[3] A. Tong, H. Dong, L. Li, *Anal. Chim. Acta* **2002**, *466*, 31.
[4] S. Sil, T. Bose, D.; Kuciauskas, J. Riskis, G. A. Caputo, V. Gulbinas, *J. Phys. Chem. B* **2010**, *114*, 16029 Roy, A. S. Chakraborti, *J. Biosci.* **2004**, *29*, 281.
[5] G. McDermott, S. M. Prince, A. A. Freer, A. M. Hawthornthwaite-Lawless, M. Z. Papiz, R. J. Cogdell, N. W. Isaaca, *Nature* **1995**, *374*, 517.
[6] A. Egawa, T. Fujiwara, T. Mizoguchi, Y. Kakitani, Y. Koyama, H. Akutsu, *Proc. Natl. Acad. Sci. USA* **2007**, *104*, 790.
[7] A. Huijser, P. L. Marek, T. J. Savenije, L. D. A. Siebbeles, T. Scherer, R. Hauschild, J. Szmytkowski, H. Kalt, H. Hahn, T. S. Balabvan, *J. Phys. Chem. C* **2007**, *111*, 11726.
[8] T. S. Balaban, *Acc. Chem. Res.* **2005**, *38*, 612.
[9] E. Zahavy, I. Willner, *J. Am. Chem. Soc.* **1996**, *118*, 12499.
[10] V. Heleg-Shabtai, T. Gabriel, I. Willner, *J. Am. Chem. Soc.* **1999**, *121*, 3220.
[11] C. M. Drain, A. Varotto, I. Radivojevic, *Chem. Rev.* **2009**, *109*, 1630.
[12] W. I. White, in *The Porphyrins, Vol. I* (Ed.: D. Dolphin), Academic Press, New York, **1978**, chap. 7, p. 303.
[13] J.-H. Fuhrhop, C. Demoulin, J. Rosenberg, C. Boettcher, *J. Am. Chem. Soc.* **1990**, *112*, 2827.
[14] L. M. Scolaro, M. Castriciano, A. Romeo, S. Patanè, E. Cefalì, M. Allegrini, *J. Phys. Chem. B* **2002**, *106*, 2453.
[15] T. Sagawa, S. Fukugawa, T. Yamada, H. Ihara, *Langmuir* **2002**, *18*, 7223.
[16] C. Li, T. Imae, *Langmuir* **2003**, *19*, 779.
[17] C. Humbert, C. Volcke, Y. Sartenaer, A. Peremans, P. A. Thiry, L. Dreesen, *Surf. Sci.* **2006**, *600*, 3702.
[18] D. Liu, W. Wu, Y. Qiu, S. Yang, S. Xiao, Q.-Q. Wang, L. Ding, J. Wang, *Langmuir* **2008**, *24*, 5052.
[19] X.-F. Wang, O. Kitao, *Molecules* **2012**, *17*, 4484.
[20] R. F. Donnelly, P. A. McCarron, D. Woolfson, *Recent Pat. Drug Delivery Formulation* **2009**, *3*, 1–7.
[21] I. Sylvain, R. Zerrouki, R. Granet, Y. M. Huang, J.-F. Lagorce, M. Guilloton, J.-C. Blaisb, P. Krausza, *Bioorg. Med. Chem.* **2002**, *10*, 57.
[22] V. Sol, F. Lamarche, M. Enache, G. Garcia, R. Granet, M. Guilloton, J. C. Blaisb, P. Krausz, *Bioorg. Med. Chem.* **2006**, *14*, 1364.
[23] M. E. El-Zaria, H. S. Ban, H. Nakamura, *Chem. Eur. J.* **2010**, *16*, 1543.
[24] S. V. Bhosale, S. V. Bhosale, M. B. Kalyankar, S. J. Langford, *Aust. J. Chem.* **2010**, *63*, 1326.
[25] S. V. Bhosale, S. V. Nalage, M. B. Kalyankar, J. M. Booth, S. K. Bhargava, S. V. Bhosale, *Supramol. Chem.* **2012**, *24*, 779.
[26] S. V. Bhosale, M. B. Kalyankar, S. V. Nalage, S. V. Bhosale, C. H. Lalander, S. J. Langford, *Supramol. Chem.* **2011**, *23*, 563.
[27] S. V. Bhosale, M. B. Kalyankar, S. V. Bhosale, S. G. Patil, C. H. Lalander, S. J. Langford, S. V. Nalage, *Supramol. Chem.* **2011**, *23*, 263.
[28] M. Ward, *Chem. Soc. Rev.* **1997**, *26*, 365.
[29] G. M. Whitesides, J. P. Mathias, C. T. Seto, *Science* **1991**, *254*, 1312.
[30] D. Philp, J. F. Stoddart, *Angew. Chem. Int. Ed. Engl.* **1996**, *35*, 1154; *Angew. Chem.* **1996**, *108*, 1242.
[31] J. K. M. Sanders in *Comprehensive Supramolecular Chemistry, Vol. 9* (Eds.: J. L. Atwood, J. E. E. Davies, D. D. MacNicol, F. Vogtle, D. N. Reinhoudt J.-M. Lehn,), Pergamon, New York **1996**, 131.
[32] D. L. Huffman, K. S. Suslick, *Inorg. Chem.* **2000**, *39*, 5418.
[33] J.-R. Dunetz, C. Sandstrom, E. R. Young, P. Baker, S. A. Van Name, T. Cathopolous, R. Fairman, J. C. de Paula, K. S. Akerfeldt, *Org. Lett.* **2005**, *7*, 2559.
[34] M. Aoudia, M. A. Rodgers, *Langmuir* **2005**, *21*, 10355.
[35] D. Kuciauskas, G. A. Caputo, *J. Phys. Chem. B* **2009**, *113*, 14439.
[36] D. V. Zaytsev, F. Xie, M. Mukherjee, A. Bludin, B. Demeler, R. M. Breece, D. L. Tierney, M. Y. Ogawa, *Biomacromolecules* **2010**, *11*, 2602.
[37] D.; Kuciauskas, J. Riskis, G. A. Caputo, V. Gulbinas, *J. Phys. Chem. B* **2010**, *114*, 16029.
[38] Q. Wang, Y. Chen, P. Ma, J. Lu, X. Zhang, J. Jiang, *J. Mater. Chem.* **2011**, *21*, 8057.
[39] E. A. Larkina, V. N. Luzgina, R. P. Evstigneeva, *Russ. J. Bioorg. Chem.* **2002**, *28*, 322.

[40] L. J. Prins, J. Huskens, F. de Jong, P. Timmerman, D. N. Reinhoudt, *Nature* **1999**, *398*, 498.
[41] S. Manchineella, V. Prathyusha, U. D. Priyakumar, T. Govindaraju, *Chem. Eur. J.* **2013**, *19*, 16615.
[42] S. S. Babu, D. Bonifazi, *ChemPlusChem* **2014**, *79*, 895.
[43] J. Zhang, R. Marega, L.-J. Chen, N.-W. Wu, X.-D. Xu, D. C. Muddiman, D. Bonifazi, H.-B. Yang, *Chem. Asian J.* **2014**, *9*, 2928.
[44] K. Yoosaf, T. Marangoni, A. Belbakra, R. Marega, E. Botek, D. Bonifazi, N. Armaroli, *Chem. Eur. J.* **2011**, *17*, 3262.
[45] K. Yoosaf, A. Belbakra, N. Armaroli, A. Llanes-Pallas, D. Bonifazi, *Chem. Commun.* **2009**, 2830.
[46] S. W. Provencher, *J. Chem. Phys.* **1976**, *64*, 2772.

Received: January 8, 2015
Published online on March 14, 2015

